SAND2013-4660C

FAST NEUTRON SPECTROSCOPY FOR MATERIALS ACCOUNTANCY OF URANIUM HEXAFLUORIDE

Scott Kiff, Erik Brubaker, Mark Gerling, Laura Kogler, Peter Marleau, Wondwosen Mengesha, and Michael Streicher
Sandia National Laboratories†
P.O. Box 969, MS 9406, Livermore, CA 94551-0969

ABSTRACT
One of the most important problems in nonproliferation is monitoring the degree of enrichment from uranium enrichment plants. Existing technologies for measuring ^{235}U enrichment in a UF_6 container (for example, a 30B cylinder) require controlled geometries for accurate measurements, which is unattractive for fielded systems. Low-energy neutrons and gammas used by current technologies have short penetration through dense UF_6, and since the UF_6 thickness near the measurement location is not known *a priori*, the current measurement techniques are sensitive to the geometry of UF_6 in the cylinder. Sandia is investigating the use of highly-penetrating fast neutrons to ascertain the UF_6 enrichment inside the cylinder. This submission focuses on the use of the neutron energy spectrum as a measure of the uranium enrichment, since the different processes that contribute to the spectrum are a function of isotopic content. A comparison of techniques including gross count rates, energy windowing, and principal component analysis will be presented, along with a discussion of the measurement concept, limitations, and simulation results.

INTRODUCTION
Safeguards activities at uranium enrichment facilities require accurate, independent measurements of uranium mass for each UF_6 cylinder with contents that are either a process input or output. Current technology tends to rely upon gamma measurements (186 keV from ^{235}U decay) or thermal neutron counting using ^{3}He detectors [1]. Both methods are sensitive to geometrical perturbations of the UF_6 within the cylinder, giving rise to potentially significant systematic measurement uncertainties; also, given the short path length of low-energy gammas and neutrons through UF_6, these methods tend to be insensitive to material in the center of the cylinder (see Figure 1). In the context of international safeguards, it is undesirable to rely upon a measurement technique that is effectively a measurement of the outer material skin; a full-volume assay is important for material balance at an enrichment facility.

Sandia is investigating the use of fast neutron spectrometers to augment the measurement capabilities surrounding UF_6 cylinder verification. Neutron spectrometry will allow for direct calculation of total mass and enrichment using two processes that generate significant neutron populations in the UF_6 [1]: spontaneous fission in ^{238}U (neutrons extending to about 10 MeV) and neutrons produced by bombardment of ^{234}U and ^{238}U decay αs upon fluorine, which terminate at about 2.5 MeV. ^{238}U mass will be proportional to the number of neutrons detected from spontaneous fission above 2.5 MeV; ^{235}U mass is reported in the literature to be proportional to ^{234}U in mass-based enrichment processes, and is determined by the neutrons counted below 2.5 MeV

† Sandia National Laboratories is a multi-program laboratory managed and operated by Sandia Corporation, a wholly owned subsidiary of Lockheed Martin Corporation, for the U.S. Department of Energy's National Nuclear Security Administration under contract DE-AC04-94AL85000.

(total counts below 2.5 MeV minus the calculated ^{238}U spontaneous fission contribution and minus the corresponding ^{238}U (α,n) rate). Figure 2 shows the contributions to the UF_6 neutron spectrum.

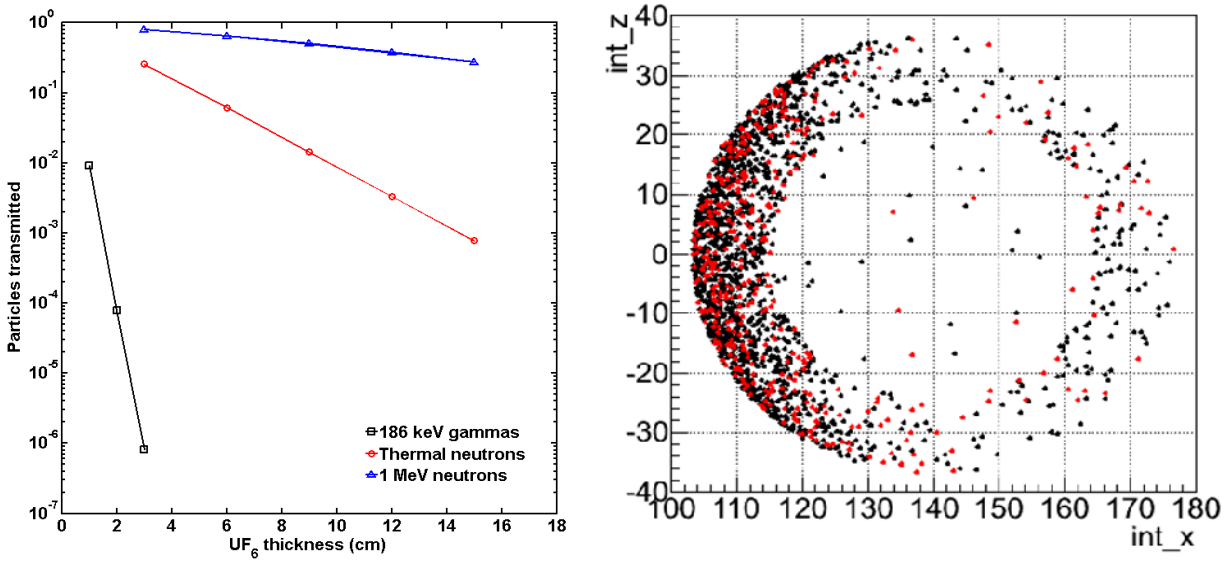

Figure 1. (Left) A calculation of particle beam transmission through a given thickness of UF_6. Induced fission is not considered in this calculation. High-energy neutrons have demonstrably superior transmission for full-volume assays. (Right) A plot of the starting locations of neutrons contributing to the measured neutron energy spectrum; in this case, the detector is a Sandia Neutron Scatter Camera placed at location int_x=0 cm. The source is a 30B cylinder containing the maximum loading of 5% enriched UF_6 distributed uniformly along the cylinder wall. Black dots correspond to neutrons generated by spontaneous fission or (α,n) processes; red dots are induced fissions. While the majority of tallied neutrons are from the material nearest the detector, events are shown to be sampled from the entire 30B cylinder.

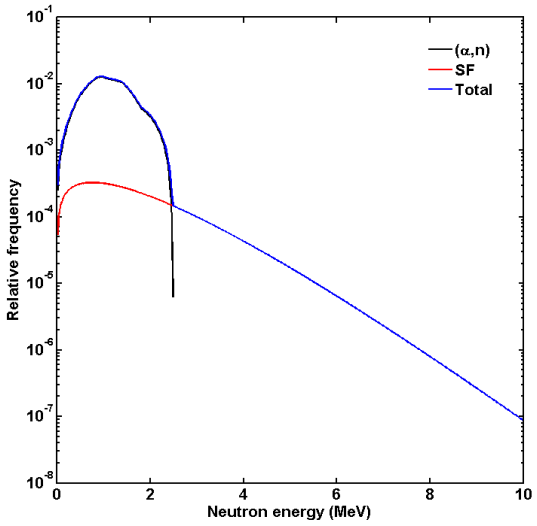

Figure 2. A plot of the neutron spectral components for 5% enriched UF_6. The ^{234}U (α,n) reaction on fluorine generates a peaked neutron spectrum that terminates abruptly near 2.5 MeV. The ^{238}U spontaneous fission spectrum peaks near this upper boundary, and extends out to about 10 MeV. This is the energy distribution of starting neutrons only—those generated by radioactive decay processes in the cylinder. Induced fission will add another term that with a distribution very similar to the spontaneous fission component.

Although the processes that generate neutrons in UF_6 samples are readily acknowledged [2], to the best of the authors' knowledge neutron spectrometry has not been directly applied as a tool to independently measure ^{238}U and ^{235}U content of 30B cylinders. This technique has two strong advantages: first, it relies upon the measurement of highly-penetrating particles, making it possible to sample the entire UF_6 volume; second, using neutron spectrometry to determine the spontaneous fission and (α,n) components provides an independent measurement enrichment and total mass.

While there are multiple viable candidate technologies for a fast neutron spectrometer, this effort has considered the Sandia Neutron Scatter Camera [3], a mature and well-characterized instrument that has been available for use by this project team. The Neutron Scatter Camera is an array of detection cells filled with Eljen EJ-309 organic liquid scintillator, which is used because its high density provides good detection efficiency, it has a fast response to events (~10 ns) that reduces dead time and pileup effects in high-rate environments, and pulse shape discrimination can be implemented to distinguish neutrons from gamma rays that can contaminate the desired signal. In the Neutron Scatter Camera, the neutron energy spectrum is often generated using the subset of events that scatters in two different cells, with each neutron's energy calculated directly as the sum of two components: the energy deposited in the first cell (calculated from the measured scintillation pulse amplitude) and the energy of the neutron as it leaves that cell, calculated from the time-of-flight between the two triggered cells. The population of neutrons that scatter only in a single cell can also be used to generate a pulse-height spectrum, the shape of which is a function of the incident neutron spectrum and is therefore still useful for analysis. This single-scatter population is generally used in the analyses described here because the number of events is greater by $O(100)$.

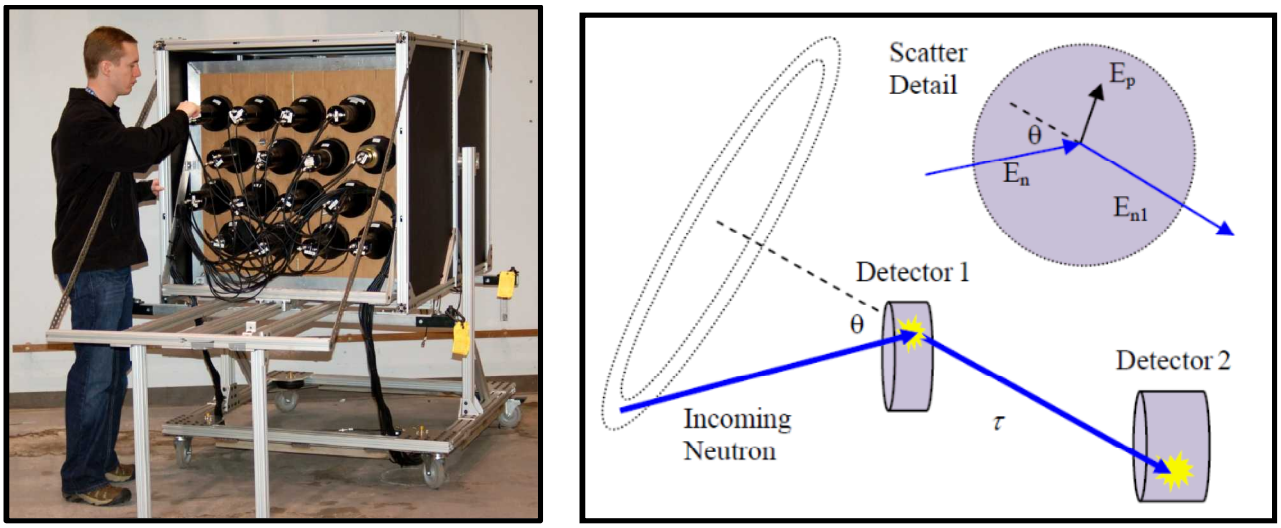

Figure 3. (Left) An author (Gerling) with the Neutron Scatter Camera. The rear of one plane containing 16 EJ-309 cells is shown; a second plane of 16 cells cannot be seen in this view. (Right) A schematic of double-scatter event reconstruction in the Neutron Scatter Camera; energy reconstruction requires the positions of Detectors 1 and 2, the energy deposited in Detector 1, and the time of flight between the trigger of each detector.

A significant body of work has been accomplished in the investigation of fast neutron spectrometry as a 30B cylinder verification technique. Simulations using detailed neutron energy sampling and Monte Carlo transport have been used to model passive neutron emissions of 30B cylinders. Studies

of detector response were used to predict the performance of the Neutron Scatter Camera (or a related variant); these calculations used detailed models benchmarked to actual measurements with the Neutron Scatter Camera. A combination of laboratory experiments and field measurements of 30B cylinders has been used to validate the simulation work.

SIMULATIONS

Previous publications [4-6] describe the simulation efforts in great detail; that information will only be summarized in this discussion. The neutron emission spectra calculated for these simulations use the isotopics presented in Berndt [1] for depleted uranium hexafluoride (DU), natural uranium (^{nat}U), and uranium enriched to 5% ^{235}U (LEU). In some cases interpolation of that isotopic data is used to generate intermediate enrichments. SOURCES 4C [7] is used to calculate the spontaneous fission and (α,n) spectral contributions. The SOURCES 4C calculated spectral contributions are presented in Figure 4.

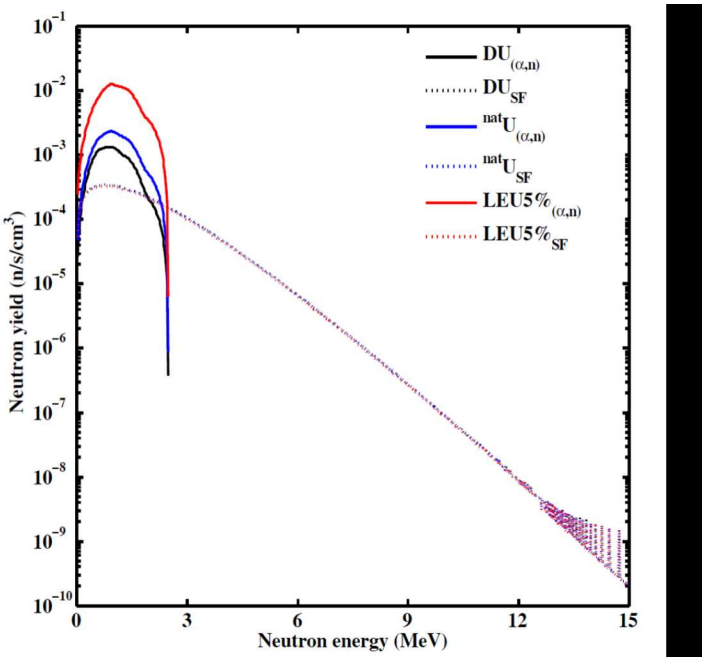

Figure 4. The (α,n) and spontaneous fission (SF) contributions to the neutron energy spectrum for three enrichment levels of UF_6, plotted separately. The spontaneous fission spectral contributions are nearly identical for each enrichment, since the total ^{238}U mass is approximately constant. However, the (α,n) contribution varies by over an order of magnitude, changing the total energy spectrum in a quantifiable manner.

To calculate the degradation of the energy spectra via scattering, capture, and induced fission in the UF_6, the SOURCES 4C spectra are inserted into an MCNP5 [8] model of a 30B cylinder [9]. This model considers a maximum loading of UF_6; in most cases, a uniform distribution of material in a thick shell is modeled. MCNP5 is used to handle the particle transport through the cylinder to the face of the detection system. At this point, source particle information is written to an intermediate file and read by Geant4 [10] to finish transport in the detector and generate the detector response. Particle transport was divided over two regions because MCNP5 was found to run much faster for the transport through the cylinder, but Geant4 provided greater flexibility in generating the detector response. Runs corresponding to 10-hour data collections were typical to ensure good counting

statistics were available throughout the entire neutron energy spectrum; sub-sampling of large data sets is easily performed to approximate shorter measurement times. Examples of the simulated measured neutron energy spectra for single-cell events in the Neutron Scatter Camera are shown in Figure 5.

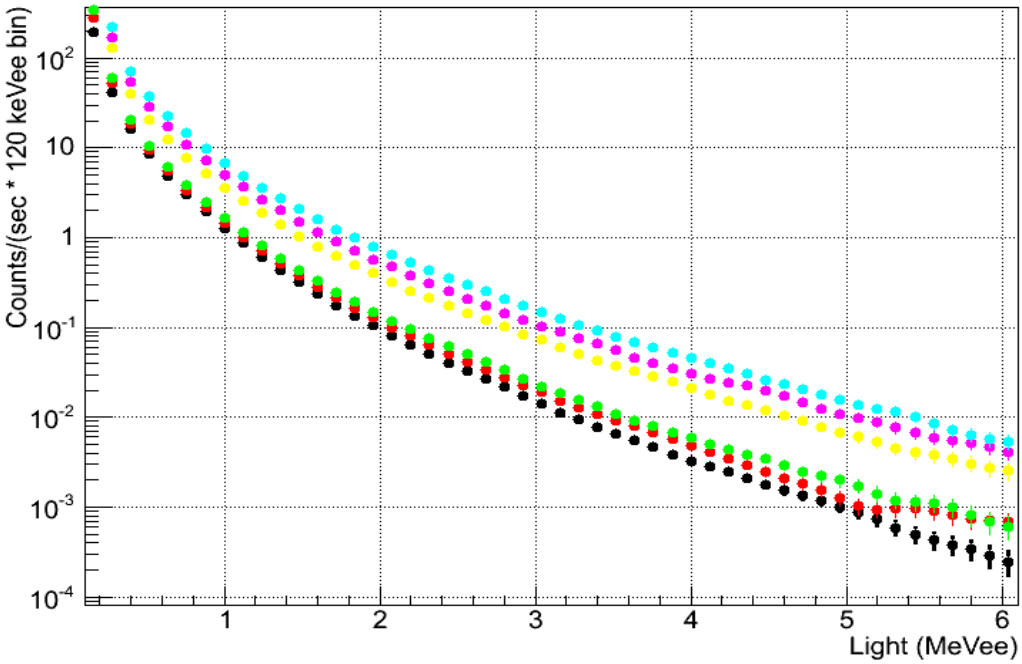

Figure 5. Calculated neutron energy spectra for single-cell measurements in the Neutron Scatter Camera. ^{235}U enrichments displayed are 0.3% (black), 0.72% (red), 1% (green), 3% (yellow), 4% (magenta), and 5% (blue).

DATA ANALYSIS

The calculated detector response pulse height spectra contain enrichment-dependent content that can be extracted during data analysis. For the simulated data, three data analysis methods have been considered. In order of least to most sophisticated, they are simple gross count rate analysis, energy spectrum windowing, and principal components analysis. All analyses operate on the same simulation data, and can therefore be compared against each other in terms of performance.

Gross Count Rate Analysis

For this data analysis effort, the shape of the energy spectrum was neglected and the analysis focused on the enrichment dependence of the measured neutron rate in the Neutron Scatter Camera cells. There is an expectation of increased neutron output with increasing enrichment due to the higher ^{234}U(α,n) output, and the increased ^{235}U induced fission rate. While gross count rate analysis is attractive because it is a simple technique, it cannot also independently estimate the mass of material in the 30B cylinder; the cylinder mass must be determined using a load cell.

Figure 6 demonstrates how the count rate is quite sensitive to the implemented energy threshold; care must be taken in choosing an appropriate threshold to balance sensitivity and measurement stability over time. Figure 7 displays measured count rates over all cells in the Neutron Scatter Camera as a function of enrichment. It is evident that the distribution of UF_6 within a 30B cylinder

(the distributions shown correspond with those defined in Berndt [1], Fig. 7) has a non-negligible effect on the measured rate, and is therefore a source of systematic uncertainty. It is believed that more sophisticated analysis techniques may reduce this systematic uncertainty term.

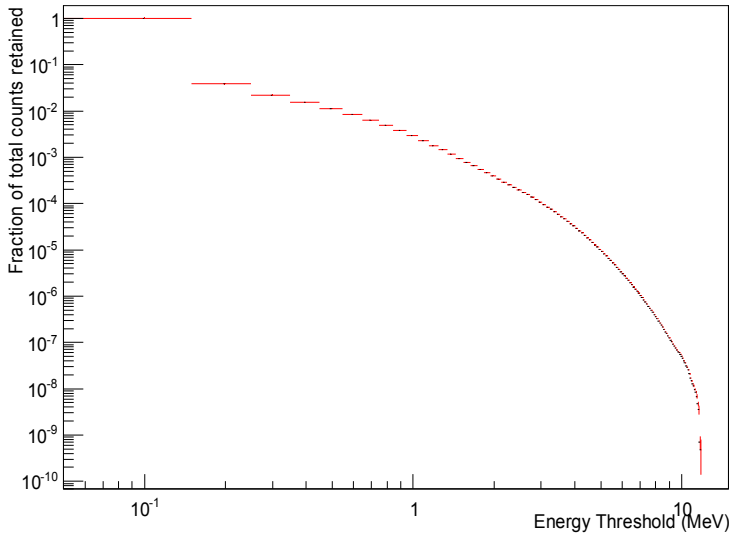

Figure 6. A demonstration of the integrated fraction of the neutron energy spectrum above a threshold energy. This indicates how much signal will be discarded as a function of threshold.

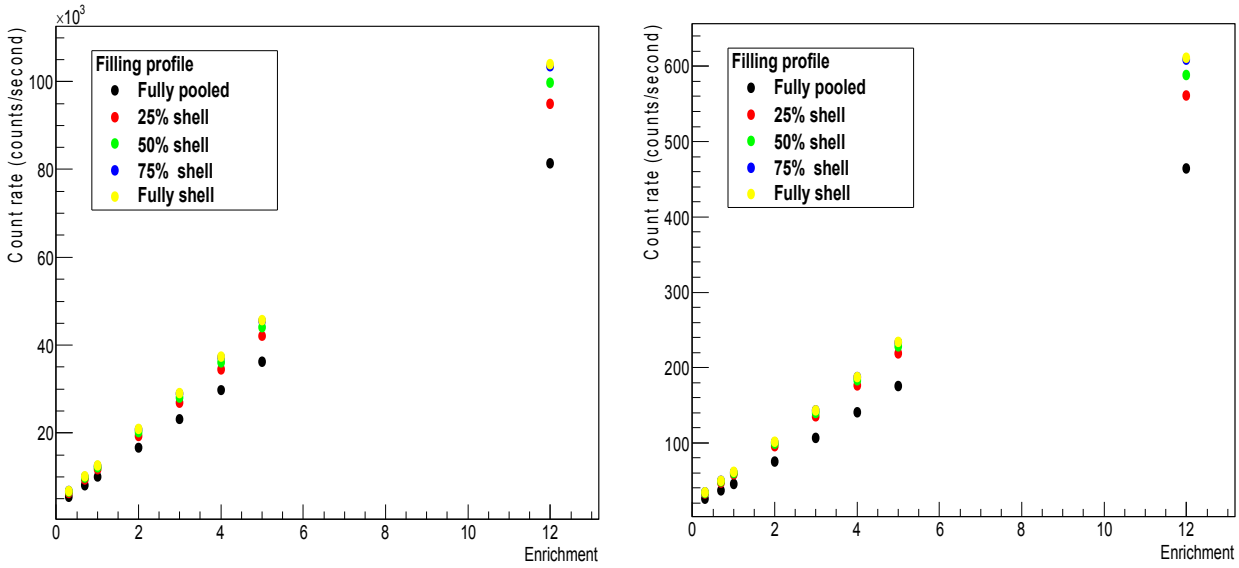

Figure 7. The total event rate in the Neutron Scatter Camera as a function of enrichment assuming a 50 keV optimistic threshold (left) and 700 keV pessimistic threshold (right). The colors represent different UF_6 distributions within the 30B cylinder, and are a source of systematic uncertainty in many 30B measurements (and probably all 30B neutron measurements).

Energy Windowing

In this analysis technique, two non-overlapping bins are used to crudely focus on key regions of the measured pulse height distribution. The bins do not have to span the entire dynamic range of the

pulse height spectrum. The position and width of these bins is optimized on a training set of data, and then applied to a different set of simulated data.

This analysis technique appears to work reasonably well, although the effect of cylinder-specific UF_6 material distribution has not been quantified (the gross counting technique was evaluated against many possible UF_6 material distributions with the 30B). It is still not clear exactly how sensitive this technique is to the subset of data used for training. Still, it appears that energy windowing may hold promise as an analysis technique.

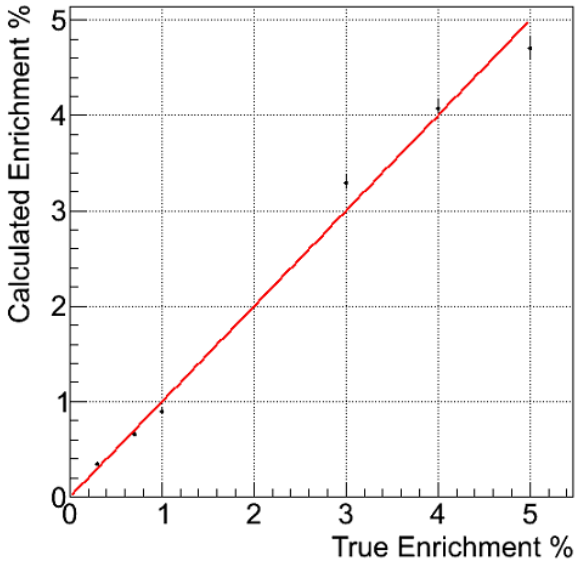

Figure 8. The estimated enrichment of simulated 30B cylinders vs. the true enrichment, as determined with the optimized energy windows.

Principal Components Analysis

Principal component analysis (PCA) is a statistical technique that transforms a set of correlated variables (here, energy bins) into uncorrelated variables called principal components (PCs). The first PC accounts for the maximum variability in the data, and each subsequent PC accounts for decreasing amounts of the variability. In this application, the energy bins have been combined in advance to form 10 much coarser bins; the purpose of this is to minimize the statistical fluctuations in each bin from one simulated spectrum to the next, thereby keeping the PCs from being trained on statistical fluctuations. This effort is being described more thoroughly in a paper being prepared for IEEE Transactions on Nuclear Science [11].

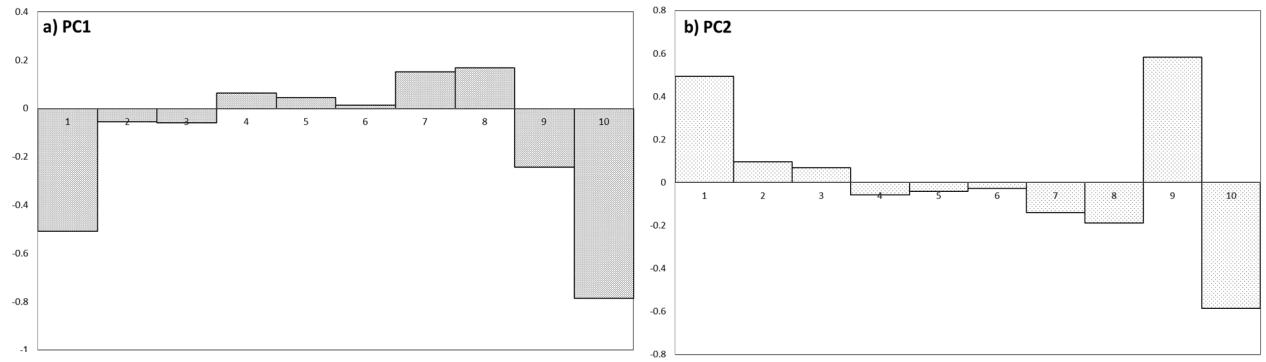

Figure 9. Eigenvectors for PC1 and PC2. The weights applied to the eigenvectors reveal the significance of the low energy group (mainly from (α, n) processes) and the high energy (>4 MeV) groups in the neutron spectra.

DISCUSSION

The presented work focuses on the use of neutron spectrometry for 30B cylinder accountancy measurements, and specifically considers the response of the Neutron Scatter Camera for this safeguards measurement application. As currently configured the Neutron Scatter Camera is optimized to locate sources in far-field imaging, and some modifications of liquid scintillator cell sizes and spacing may be required for 30B cylinder enrichment measurements. It may very well be that the Neutron Scatter Camera is not the ideal neutron spectrometer for this application, as it currently has a detection threshold for single-scatter events near 500 keV and double-scatter events near 1 MeV—as seen in Figure 4, this high threshold cuts out a large portion of events, which may reduce the measurement accuracy or increase the required measurement time relative to a spectrometer with a lower detection threshold. In addition, 30B cylinders emit far more gamma rays than neutrons, and the gamma sensitivity of liquid scintillators can result in pulse pileup challenges during field measurements. A survey of other neutron spectrometry technologies is warranted, given the promise of this measurement technique.

Neutron spectrometry is not the only concept being explored for passive neutron measurements of 30B cylinders. Other efforts rely on the moderation of neutrons for detection with ^{3}He counters [12], or conversion of neutrons into high-energy photons in the steel cylinder wall [2]. It is important to note that all of these efforts are examining the same population of neutrons; it is the measurement and analysis techniques that differ. The authors believe direct measurement of fast neutron signatures in general (including the proposed spectrometry measurement) are attractive because the unperturbed neutron field carries useful information on enrichment, mass, and material distribution; other techniques that rely on conversion or moderation destroy some of the information contained in the emitted neutron field for the purpose of measurement. While liquid scintillators are not always ideal detectors, they allow for construction of high-efficiency systems at reasonable cost.

There are, of course, limitations to this measurement concept. The measurement precision is unlikely to ever challenge the performance of the enrichment meter [13], although the point of the neutron spectrometer is to reduce potential systematic uncertainties, which could potentially be large with the enrichment meter in uncontrolled measurement configurations. Also, the neutron spectrometry technique relies upon a well-characterized relationship between ^{234}U and ^{235}U isotopic fractions; however, the introduction of reprocessed uranium may complicate the analysis because

the isotope ratios will be different after sufficient neutron irradiation in a reactor. Down-blended material may introduce similar isotopic complications. These concerns are not unique to the proposed neutron spectrometry enrichment measurement: the gamma ray flux is a concern for all detectors except those that are truly gamma-insensitive (such as ^{3}He proportional detectors), and the reprocessed fuel will be a potential complication for any passive neutron measurement.

Finally, it is worth mentioning some minor benefits of utilizing the Neutron Scatter Camera for the neutron spectrometry enrichment measurement. The Neutron Scatter Camera is capable of neutron imaging, and it is possible to reject backgrounds—either a natural background or from nearby 30B cylinders—by performing neutron imaging during the measurement and rejecting neutrons that originate outside the region occupied by the cylinder being interrogated. Also, neutron imaging can potentially be used to image the UF_6 distribution within a 30B cylinder, which could provide a safeguards verification tool allowing inspectors to determine whether the cylinder internal volume matches the expectation for size, geometry, and material distribution.

CONCLUSIONS

This paper explored three data analysis methods for extracting enrichment information from the measured neutron energy spectrum. Of the three analysis techniques considered, it seems that each one can correlate its primary metric to UF_6 isotopic enrichment. The simplest technique is a measurement of the gross count rate in the fast neutron detector; the measured rate is a function of enrichment, but requires an independent measurement of cylinder mass and has significant systematic uncertainty introduced by the UF_6 distribution within the 30B. The PCA technique is much more complicated, but depending upon the training set used for the technique, may be able to remove much of this systematic uncertainty. Energy windowing is a simple way of exploiting features in the measured pulse height spectrum, but systematic uncertainties have not been explored with this technique.

In summary, this paper has provided the basis for a full-volume uranium enrichment measurement using neutron spectrometry. Simulations of 30B cylinder emissions and detailed detector response have demonstrated that the measured neutron energy spectrum contains features that can be associated with enrichment. This measurement technique provides a way to sample the full volume of a 30B cylinder, which is an important capability that is currently nonexistent in 30B NDA techniques.

REFERENCES

[1] R. Berndt, E. Franke, P. Mortreau, Nucl. Instr. and Meth. A (2010), doi: 10.1016/j.nima.2009.10.060

[2] E.K. Mace, L.E. Smith, Nucl. Instr. and Meth. A (2010), doi:10.1016/j.nima.2010.09.149

[3] J. Brennan *et al.*, IEEE Trans. Nucl. Sci. (2011), doi: 10.1109/TNS.2011.2163192

[4] S.D. Kiff, P. Marleau, and R.L. Cooper. "Fast Neutron Signatures for Uranium Hexafluoride Enrichment Measurements." *Proceedings of the INMM 52nd Annual Meeting*. Palm Desert, CA, July 17-21, 2011. Vol. 3, pg. 2214-2221.

[5] Scott D. Kiff, Peter Marleau, and Michael Streicher, "Uranium Enrichment Measurements Using Neutron Spectrometry." *Transactions of the American Nuclear Society.* Washington, D.C., Oct. 30-Nov. 3, 2011. Vol. 105, pg. 339-340.

[6] S. Kiff, Erik Brubaker, Mark Gerling, Peter Marleau, Wondwosen Mengesha, and Michael Streicher. "Fast Neutron Imaging for Materials Accountancy of Uranium Hexafluoride." *Proceedings of the INMM 53rd Annual Meeting*. Orlando, FL, July 15-19, 2012.
[7] W.B. Wilson *et al.*, "SOURCES 4C: A Code for Calculating (alpha,n), Spontaneous Fission, and Delayed Neutron Sources and Spectra," LA-UR-02-1839 (2002).
[8] F.B. Brown *et al.*, "MCNP VERSION 5," LA-UR-02-3935 (2002).
[9] R.I. Reynolds *et al.*, "American National Standard for Nuclear Materials—Uranium Hexafluoride—Packaging for Transport," ANSI N14.1-2001 (2001).
[10] S. Agostinelli *et al.*, Nucl. Instr. and Meth. A (2003), doi:10.1016/S0168-9002(03)01368-8
[11] W. Mengesha, M. Gerling, S.D. Kiff, P. Marleau, and E. Brubaker, "Application of principal component analysis for UF6 enrichment verification in storage cylinders," in preparation for submission to *IEEE Trans. Nucl. Sci.*, 2013.
[12] K.A. Miller, M.T. Swinhoe, H.O. Menlove, J.B. Marlow, "Status Report on the Passive Neutron Enrichment Meter (PNEM) for UF_6 Cylinder Assay," Los Alamos technical report LA-UR-12-21058.
[13] ASTM Standard C1514, "Standard Test Method for Measurement of ^{235}U Fraction Using Enrichment Meter Principle," ASTM International, West Conshohocken, PA, 2008, DOI: 10.1520/C1514-08, www.astm.org.